

# Reaction of HO and DO with 2-vinylfuran

M. Wollenhaupt, J. Williams and J. N. Crowley\*

Max-Planck-Institut für Chemie, Division of Atmospheric Chemistry, Postfach 3060, 55020, Mainz, Germany. E-mail: crowley@mpch-mainz.mpg.de

Received 7th July 2003, Accepted 21st August 2003

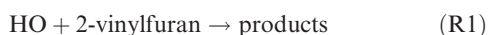
First published as an Advance Article on the web 15th September 2003

The rate constants for the reactions of the hydroxyl radical, HO and DO, with 2-vinylfuran ( $k_1$  and  $k_2$ ) were measured at  $295 \pm 2$  K using the method of pulsed laser photolytic generation of HO or DO, combined with pulsed laser induced fluorescence detection. For DO, mono-exponential decay profiles were observed, enabling a simple analysis to extract a value of  $k_2 = (8.8 \pm 0.9) \times 10^{-11} \text{ cm}^3 \text{ molecule}^{-1} \text{ s}^{-1}$ . In contrast, the decay of HO was complex, due to its regeneration in secondary reactions, and was analysed using a multi-exponential expression that enabled a rate constant of  $k_2 = (9.0 \pm 1.0) \times 10^{-11} \text{ cm}^3 \text{ molecule}^{-1} \text{ s}^{-1}$  to be extracted. The different behaviour of HO and DO provides clues to the reaction mechanism, which involves ring opening and a rearrangement/HO-elimination step. As part of this work the UV-absorption spectrum of 2-vinylfuran is also reported.

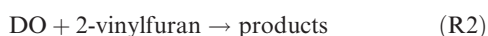
## 1 Introduction

The degradation of the vast majority of both natural and anthropogenic trace gases in the atmosphere is initiated by the hydroxyl radical, HO, making studies of its reactions critical to our understanding of trace gas lifetimes and atmospheric composition. The motivation to investigate the reaction between HO and 2-vinylfuran (furylethylene,  $\text{C}_6\text{H}_6\text{O}$ ) was provided by documentation of its emission by vegetation<sup>1</sup> and by mass spectrometric measurements of trace gases over the tropical rainforest in Surinam.<sup>2</sup> Generally, furans are emitted to the atmosphere by biomass burning,<sup>3–5</sup> and degradation of biogenics.<sup>6</sup>

There are no available data that describe the potential fate of 2-vinylfuran in the atmosphere, although the fact that reaction of HO with other furans is rapid, indicated that this is a potentially significant loss process that needed to be characterised in order to calculate its lifetime.



In this work we present laboratory measurements of the kinetics of the reaction between both HO and DO radicals with 2-vinylfuran at room temperature. The use of DO as well as HO enabled us to derive a mechanistic description of the elementary steps involved in the reaction, based on the unexpected observation of HO reformation.



## 2 Experimental

The experimental investigation of the title reaction was carried out using the pulsed laser photolysis-pulsed laser induced fluorescence (PLP-PLIF) technique in which hydroxyl radicals are generated by pulsed photolysis of suitable precursors on time scales that are short compared to their subsequent decay, and are detected by pulsed laser induced fluorescence. The experimental set-up for PLP-PLIF has been described previously<sup>7</sup> and is described only briefly here.

### 2.1 Pulsed laser photolysis-pulsed laser induced fluorescence

The experiments were carried out using a double jacketed reactor of volume *ca.* 500 cm<sup>3</sup>. Gas mixtures entered the reactor *ca.* 15 cm upstream of the photolysis region to ensure thermal equilibrium with the walls of the vessel, and were pumped out through ports in the baffle arms, and in front of the fluorescence collection lens. The cell temperature ( $295 \pm 2$  K) was measured by using a J-type thermocouple that could be inserted into the reaction volume where the focus of the telescopic lens system and the laser beams intersect. The pressure in the cell, monitored with 10, 100 and 1000 Torr capacitance manometers, was held constant at 40 Torr, using Ar as bath gas. Typical flow rates, regulated using calibrated mass flow controllers, were between 300 and 400 standard cm<sup>3</sup> min<sup>-1</sup>, (sccm), resulting in linear gas velocities in the reaction cell of *ca.* 30 cm s<sup>-1</sup>, ensuring that a fresh gas sample was photolysed at each laser pulse, and preventing build up of products.

HO radicals were generated from suitable precursors (see below) by the *ca.* 20 ns pulse of an excimer laser at 351 nm with a repetition rate of 10 Hz. Fluorescence from HO was detected by a photomultiplier tube (PMT) filtered by 309 nm interference filter and a BG 26 glass cut off filter, and recorded using a gated charge integrator. Excitation of the HO  $\text{A}^2\Sigma$  ( $v' = 1$ )  $\leftarrow$   $\text{X}^2\Pi$  ( $v = 0$ ), transition at 282 nm was achieved using the frequency doubled emission from a Nd-YAG pumped dye laser (Rhodamine 6G). The analogous wavelength for DO was 286.7 nm.

HO and DO decay profiles were constructed by incrementing stepwise (at 10 Hz) the delay between the excimer and dye lasers. The sensitivity of this set up to HO was estimated by photolysis of a known concentration of HO precursor (*e.g.*,  $\text{H}_2\text{O}_2$ ) with a known laser fluence. The detection limit was found to be *ca.*  $10^8 \text{ cm}^{-3}$  for a S/N = 1 (20 scans).

### 2.2 Generation of HO and DO radicals

Hydroxyl radicals were generated by the 351 nm dissociation of either HONO (for HO) or DONO (for DO). Typically, laser fluences of 2–15 mJ cm<sup>-2</sup> per pulse were used to generate between  $10^{10}$  and  $10^{11}$  HO cm<sup>-3</sup> from about  $5 \times 10^{13}$  molecules cm<sup>-3</sup> of HONO, the concentration of which could be

monitored using UV-absorption spectroscopy in a separate cell, linked serially in flow with the main reactor (see below).



The use of shorter laser wavelengths (193 and 248 nm) and HO precursors such as  $\text{H}_2\text{O}_2$  or  $\text{HNO}_3$  was precluded by the strong optical absorption of 2-vinylfuran, and the resultant intense, long-lived fluorescence signal (either from 2-vinylfuran itself or excited radical fragments), which obscured that of HO.

### 2.3 Optical absorption measurements of 2-vinylfuran

The concentration of 2-vinylfuran was determined by on-line optical absorption, whereby the absorption of UV light was determined in two separate absorption cells (at room temperature) linked serially in flow both before and after the reactor. Absorption measurements over a pathlength of 174 cm (upstream of the reactor) were conducted between *ca.* 200 and 300 nm using a diode array spectrograph at a resolution of 0.5 nm and converted to concentrations by least-squares fitting to a reference UV absorption spectrum measured in this laboratory (Fig. 1). Absorption at 253.65 nm was determined in a 44 cm absorption cell downstream of the reactor. Corrections for molecular density changes due to the difference in pressure (usually less than 1%) and temperature between the two absorption cells and the reactor were made to calculate the concentration of 2-vinylfuran in the reactor. A calibration spectrum of 2-vinylfuran was obtained in the same apparatus (*i.e.* diode-array spectrograph, analysis lamp, *etc.*) by measuring the optical density (OD) due to static mixtures of 2-vinylfuran in Ar following a single dilution step of *ca.* 1 : 1000. Good Beer–Lambert linearity [eqn. (1)] was observed in the plot of OD *versus* concentration of 2-vinylfuran up to  $1.25 \times 10^{14}$  molecules  $\text{cm}^{-3}$ , which also covers the range used in the kinetic

measurements (see Fig. 1).

$$\text{OD}(\lambda) = \ln\{I_0(\lambda)/I(\lambda)\} = \sigma(\lambda) l [\text{2-vinylfuran}] \quad (1)$$

where  $I_0$  and  $I$  are the analysis light intensities in the absence and presence of 2-vinylfuran, respectively,  $\sigma(\lambda)$  is the absorption cross-section (in  $\text{cm}^2 \text{ molecule}^{-1}$ ) and [2-vinylfuran] is the concentration of 2-vinylfuran (in molecules  $\text{cm}^{-3}$ ). The spectrum of 2-vinylfuran displayed in Fig. 1 is the average of 5 separate determinations at different concentrations which showed variations of less than 2% close to the maximum absorption at *ca.* 250 nm where cross-sections are of the order of  $6 \times 10^{-17} \text{ cm}^2 \text{ molecule}^{-1}$ . The uncertainty associated with the cross-sections depends mainly on the purity of the 2-vinylfuran and the accuracy of the dilution step, and is estimated as *ca.* 10%. As shown below, this ultimately limits the accuracy of the rate constants obtained.

Once the absorption spectrum between 205 and 300 nm had been obtained, a flowing mixture of 2-vinylfuran in Ar was passed through the 174 cm absorption cell into the 44 cm absorption cell which was equipped with a low pressure, Pen-ray Hg lamp as a light source, and with transmission and reference photodiodes for monitoring light intensity. The lamp was filtered with a  $254 \pm 5$  nm interference filter to isolate the main Hg emission line. Simultaneous measurement of 2-vinylfuran concentration in the 174 cm cell, and absorption in the 44 cm cell (see lower image in Fig. 1) enabled the cross-section of 2-vinylfuran at the 253.65 nm Hg line to be determined as  $4.86 \times 10^{-17} \text{ cm}^2 \text{ molecule}^{-1}$ . As a cross-check, we note that this value compares very well with the value of  $4.91 \times 10^{-17} \text{ cm}^2 \text{ molecule}^{-1}$  obtained at  $253.6 \pm 0.4$  nm in the diode array spectrum, where slight differences are expected due to inaccuracies in the wavelength calibration and low spectral resolution of the diode array. We are not aware of any previous determinations of this cross-section, to which we can compare our results.

### 2.4 Chemicals

Samples of 2-vinylfuran (> 95%, synthesised by the reaction of furfuraldehyde with either methylenetriphenylphosphorane or trimethylsilylmagnesium chloride) were kindly provided to us by Elaine Frary (Department of Chemistry, University of Sheffield, England), and used without further purification. HONO (DONO) was prepared by the drop-wise addition of concentrated  $\text{H}_2\text{SO}_4$  to a 0.1 M sample of  $\text{NaNO}_2$  in  $\text{H}_2\text{O}$  ( $\text{D}_2\text{O}$ ), and was eluted from solution in a small flow of Ar that transported it into the absorption cells and reactor. For experiments using DONO, the absorption cells and reactor were passivated with a  $\text{D}_2\text{O}$  flow to reduce H–D exchange with surface adsorbed  $\text{H}_2\text{O}$ . Despite this, the DONO source always contained a significant HONO impurity. Ar (5.0) was used without further purification.

## 3 Results

Below, we present the results of the kinetic investigations of the HO and DO reactions with 2-vinylfuran. As the interpretation of the data obtained with DO was much simpler than for HO, we begin by first discussing these results, before comparing and contrasting to the more complex behaviour seen for HO.

### 3.1 DO + 2-vinylfuran

Deuterated hydroxyl radicals (DO) were generated at low concentrations compared to 2-vinylfuran (the excess reactant) with  $[\text{2-vinylfuran}]/[\text{DO}]_0 = 10^2 - 10^4$ , and their decay profiles are expected to be exponential according to:

$$\ln([\text{DO}]_t/[\text{DO}]_0) = -(k_2[\text{2-vinylfuran}] + c)t \quad (2)$$

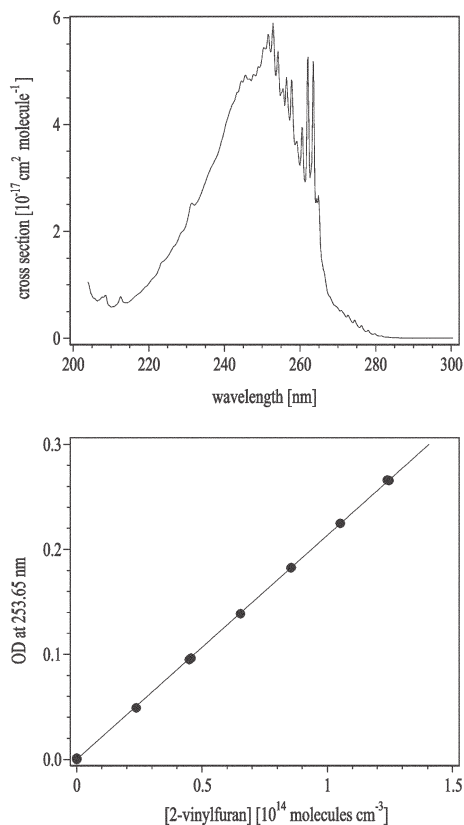


**Fig. 1** Absorption spectrum (200–300 nm, spectral resolution of 0.5 nm) of 2-vinylfuran at 296 K. The lower image shows the optical density at 253.65 nm (Hg line) *versus* 2-vinylfuran concentration. The slope results in  $\sigma(253.65 \text{ nm}) = 4.86 \times 10^{-17} \text{ cm}^2 \text{ molecule}^{-1}$ .

where  $[\text{DO}]_0$  is the initial DO concentration,  $[\text{DO}]_t$  is the concentration of DO at time  $t$  after the excimer laser pulse,  $[\text{2-vinylfuran}]$  is the concentration of 2-vinylfuran (all concentrations in molecules  $\text{cm}^{-3}$ ),  $k_2$  is the rate constant ( $\text{cm}^3 \text{ molecule}^{-1} \text{ s}^{-1}$ ) for reaction of DO with 2-vinylfuran, and  $c$  is a first order decay constant ( $\text{s}^{-1}$ ) that accounts for diffusion of DO from the detection zone, and reaction with HONO, DONO and impurities. Exponential decays (over about 3 orders of magnitude change in DO concentration) were indeed observed for experiments in which DO was employed, as illustrated by the data in Fig. 2. The pseudo-first order rate decay constant,  $k'(\text{DO})$ , is determined from the slopes and is related to the bimolecular rate constant by:

$$k'(\text{DO}) = k_2 [\text{2-vinylfuran}] + c \quad (3)$$

For a fixed concentration of 2-vinylfuran,  $k'(\text{DO})$  was not influenced by variation in the excimer laser fluence over a factor of *ca.* 7, precluding the presence of a significant secondary loss process for DO. The parameter  $[\text{2-vinylfuran}]$  was obtained from the online measurements of absorption by 2-vinylfuran in both the 174 and 44 cm absorption cells, which were conducted simultaneously with measurement of the DO decay. The deviation in concentration of 2-vinylfuran using these two methods was generally less than 3% ruling out significant loss of 2-vinylfuran in transport through the reactor. Concentration estimations were also made from the partial flow of 2-vinylfuran, the total flow and pressure, and the mixing ratio of 2-vinylfuran in its storage bulb. With this method, the concentrations agreed to within 5–10% of those measured optically, but are considered less accurate.

The plot of  $k'(\text{DO})$  versus  $[\text{2-vinylfuran}]$ , as shown in Fig. 3, defines the bimolecular rate constant as  $(8.8 \pm 0.1) \times 10^{-11} \text{ cm}^3 \text{ molecule}^{-1} \text{ s}^{-1}$  where the errors are  $2\sigma$  precision only. The high precision in determining  $k'(\text{DO})$  (statistical errors of <1%) and the low scatter in Fig. 2 means that the uncertainty related with this rate constant stems almost entirely from the determination of the concentration of 2-vinylfuran. The error associated with the least squares fitting of 2-vinylfuran absorption to the reference spectrum is also negligible (<1%), leaving only the uncertainty in the cross-section as source of error. As discussed above, this is related to purity and dilution accuracy, and is estimated as *ca.* 10%.

### 3.2 HO + 2-vinylfuran

For HO, a rather different picture was obtained and, as illustrated in Fig. 4, the decay profiles of HO in various excess

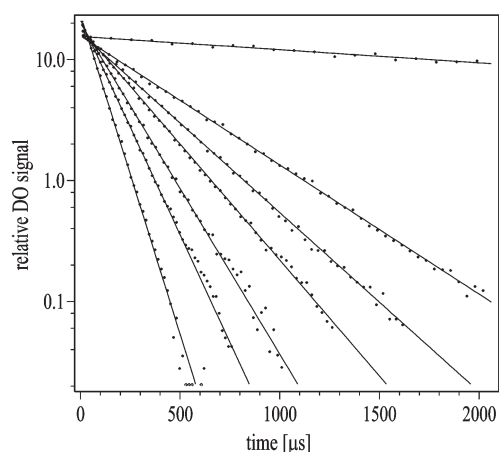


**Fig. 2** Decay of DO in the presence of various excess concentrations of 2-vinylfuran. The photolysis of DONO at 351 nm was used as a DO source. The concentrations of 2-vinylfuran were 0, 2.54, 3.63, 4.72, 6.82, 8.89 and  $12.9 \times 10^{13}$  molecules  $\text{cm}^{-3}$  in going from the slowest to the fastest decay.

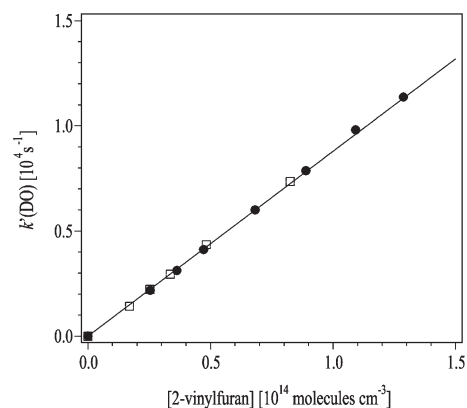


**Fig. 3** Plot of pseudo first order decay constant,  $k'(\text{DO})$ , versus concentration of 2-vinylfuran. The different symbols are data from different 2-vinylfuran samples. The data have been corrected by subtracting the measured value of  $k'(\text{DO})$  in the absence of 2-vinylfuran. Statistical errors are smaller than the symbols.

concentrations of 2-vinylfuran were clearly not mono-exponential, or indeed bi-exponential. The HO decays are characterised by an initially rapid decay, which is approximately exponential at high  $[\text{2-vinylfuran}]$ , and a much slower exponential decay at long reaction times. At intermediate reaction times and high  $[\text{2-vinylfuran}]$ , there is a distinct inflexion point. These decay profiles are strongly suggestive of a process occurring in which HO is regenerated *via* the formation and subsequent decomposition (to release HO) of a reaction product. The absence of such features when DO was detected, suggests that this can not be explained by invoking an approach to equilibrium involving, *e.g.*, formation and re-dissociation of a 2-vinylfuran-HO adduct with an additional loss process to deplete its equilibrium concentration. Evidence for a mechanism in which an initially formed radical product can rearrange before decomposing to release a hydroxyl radical was obtained in experiments in which DO was generated and reacted with 2-vinylfuran, but with the probe laser set up for HO (282 nm) detection. In this case, we were able to observe the formation of HO, initiated by the reaction of DO with 2-vinylfuran, as displayed in Fig. 5. The initially decreasing HO signal is due to HO formed in the photolysis of HONO impurity in the DONO sample. We shall speculate on the nature of the intermediate and the mechanism by which HO is reformed in this system later.

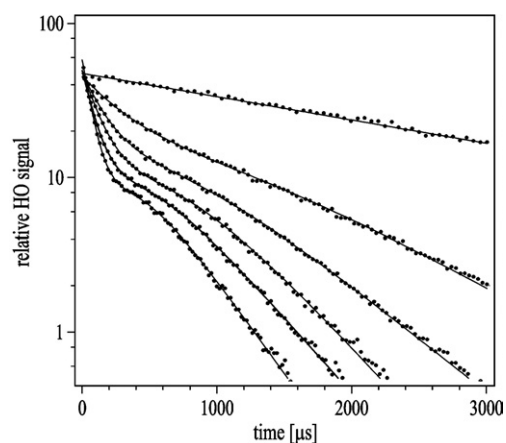


**Fig. 4** Decay of HO in the presence of various excess concentrations of 2-vinylfuran. Photolysis of HONO at 351 nm was used as HO source. The concentrations of 2-vinylfuran were 0, 2.36, 4.60, 6.69, 8.75 and  $12.7 \times 10^{13}$  molecules  $\text{cm}^{-3}$  in going from the slowest to the fastest decay.

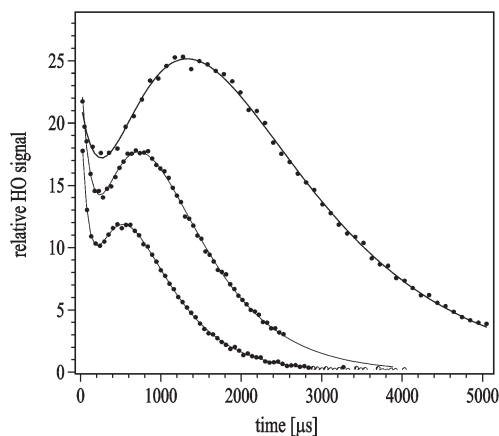


**Fig. 5** Formation and decay of HO in the presence of various excess concentrations of 2-vinylfuran. In these experiments DONO (plus HONO impurity) was photolysed at 351 nm, and LIF from HO was monitored. The concentrations of 2-vinylfuran were 1.69, 4.83 and  $8.25 \times 10^{13}$  molecules  $\text{cm}^{-3}$  for the upper, middle and lower curves, respectively.

The shapes of the HO decays shown in Figs. 4 and 5 were found not to be dependent on the excimer laser fluence (varied by a factor of 5), and therefore on the initial concentration of HO. This rules out that secondary reactions between initial radical products (which should display a quadratic dependence on HO) play an important role, and enables us to fit the data using a tri-exponential analytical expression (4). This expression includes a combined rate constant representing the sum of pseudo-first order decay constants for the (initial) elementary steps of addition of OH to various sites of 2-vinylfuran, the rate constant for decomposition of one (or more) of these initially formed radicals to its isomer, and the rate constant for decomposition of this isomer to OH.

$$[\text{HO}]_t/[\text{HO}]_0 = P\exp(-pt) + Q\exp(-qt) + R\exp(-rt) \quad (4)$$

The solid lines in Figs. 4 and 5 are the results of least squares fitting each data set to eqn. (4). The initial decay rate of HO,  $k'(\text{HO})$ , can be obtained exactly from expression (5):

$$k'(\text{HO}) = (pP + qQ + rR)/(P + Q + R) \quad (5)$$

where the parameters  $p$ ,  $P$ ,  $r$ ,  $R$ ,  $q$  and  $Q$  are all returned from the fit of eqn. (4) to the decays. The rate constant  $k_1$  can then be obtained from plots of  $k'(\text{HO})$  versus [2-vinylfuran] as shown in Fig. 6. This yields a rate constant  $k_1 = 9.0 \times 10^{-11}$   $\text{cm}^3 \text{ molecule}^{-1} \text{ s}^{-1}$  which is very close to that of  $k_2$  for DO.

A simpler analysis can be conducted by fitting a single exponential to the data in the time period shortly after the HO is generated. The disadvantage of this method is that it is restricted to data sets with high 2-vinylfuran for which the decay has mono-exponential character over an extended time period, and will generally result in an underestimation of the true first order decay constant. Analysis of the present data in this manner resulted in values of  $k'(\text{HO})$  that were consistently smaller than those obtained by eqns. (4) and (5) by 10 to 15%, with the largest deviation found for those decays in lower concentrations of 2-vinylfuran. Nevertheless, this agreement is reasonable, and confirms that we are extracting the correct pseudo-first order decay constant,  $k'$ , from the complex, multi-exponential analysis in order to derive the bimolecular rate coefficient,  $k_1$ .

## 4 Discussion

Within experimental error, our measured rate constants,  $k_1$  and  $k_2$ , for the reaction of HO and DO with 2-vinylfuran

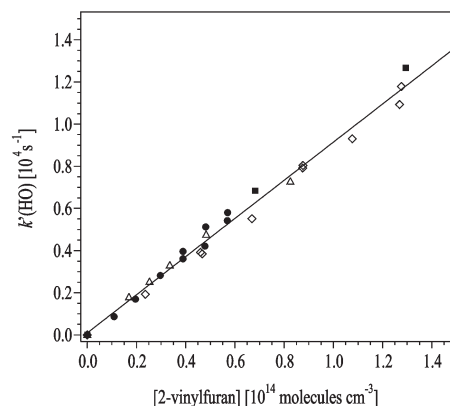


**Fig. 6** Plot of pseudo-first order decay constant,  $k'(\text{HO})$ , versus concentration of 2-vinylfuran. The different symbols are data from different 2-vinylfuran samples. The data have been corrected by subtracting the measured value of  $k'(\text{HO})$  in the absence of 2-vinylfuran. Due to the multi-exponential fitting routine, a simple error estimation was not possible for each data point, hence error bars are not shown.

are identical. This result is expected as only very small changes in rate constant are expected upon deuteration of HO as the H–O bond is unlikely to be broken in the initial step. Note that both  $k_1$  and  $k_2$  describe the overall loss of HO, which likely involves addition at a number of different sites. The rate constants for reaction of hydroxyl for several other furans have been previously measured, and all found to be rapid, with rate constants (units of  $\text{cm}^3 \text{ molecule}^{-1} \text{ s}^{-1}$ ) of  $4.1 \times 10^{-11}$  for furan,<sup>8–10</sup>  $6.2 \times 10^{-11}$  for 2-methylfuran,<sup>8</sup>  $9.3 \times 10^{-11}$  for 3-methylfuran,<sup>6</sup>  $10.8 \times 10^{-11}$  for 2-ethylfuran<sup>8</sup> and  $13.2 \times 10^{-11}$  for 2,5-dimethylfuran.<sup>8</sup> The trend within these rate constants shows that electron donating substituents have a positive induction effect and enhance the rate of the addition of HO to the  $\Pi$  system. Comparison between 2-methylfuran and 3-methylfuran and also between furan-2-aldehyde and furan-3-aldehyde shows that substituents at the 3-position appear to have a stronger enhancing effect than at the 2-position.<sup>11</sup> The enhanced rate constant for 2-vinylfuran compared to furan is due to the extra double bond external to the aromatic ring that can provide both stabilisation of the initial adduct formed, and an extra addition site.

From our measurement of a rate constant of  $k_1 \approx 9 \times 10^{-11}$   $\text{cm}^3 \text{ molecule}^{-1} \text{ s}^{-1}$  and an approximate, diurnally averaged concentration of *ca.*  $1 \times 10^6$  HO  $\text{cm}^{-3}$  in the lower troposphere, we can estimate the lifetime of 2-vinylfuran as *ca.* 3 h. Comparison with previous studies on other furans (no data is available for 2-vinylfuran) suggests that the rate constant with  $\text{NO}_3$  will be lower than that for HO, but may represent a modest sink at night-time.<sup>12</sup>

In the following, we discuss possible mechanisms for the reaction of hydroxyl with 2-vinylfuran. In the absence of a detailed product study we can deduce mechanistic information only from our kinetic observations, and the mechanisms we suggest below are somewhat speculative, and do not attempt to give a complete picture of the various possible reaction pathways, but rather focus on the issue of HO regeneration. However, as the rate constant for reaction of both DO and HO with 2-vinylfuran is comparable to those found for addition of hydroxyl radicals to double bonded systems rather than abstraction of an H-atom from C–H groups, we can assume that the first step is addition of DO across either the double bond external to the aromatic ring, or to the ring itself. The favoured position at the ring is expected to be that associated with the largest number of resonant structures, *i.e.* addition at the ortho position to form the 2-vinyl-5-hydroxyfuran radical (Fig. 7, step a). Two pieces of information provide clues to the fate of this radical. Firstly, our observation of non-exponential

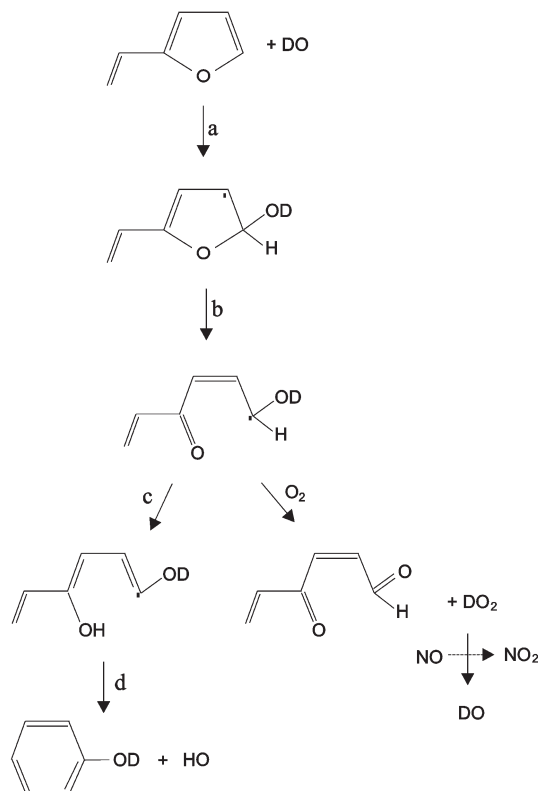


**Fig. 7** A potential reaction scheme to explain the formation of HO when DO reacts with 2-vinylfuran in the absence of  $\text{O}_2$  (a–d), and the non-exponential decays of DO indicating its re-formation following reaction with 2-vinylfuran in the presence of  $\text{O}_2$  (a, b, then reaction with  $\text{O}_2$ ).

HO decays and HO release when DO reacts with 2-vinylfuran can be compared to the reaction with furan, where such effects were not observed<sup>9</sup> which suggests that the external double bond may be requisite to HO regeneration. Second, information concerning the reaction mechanism could be gained in a limited set of experiments in which the influence of  $\text{O}_2$  on the HO and DO decay profiles was examined. Fig. 8 displays DO profiles obtained in the absence of  $\text{O}_2$  (curve A, exponential decay) and in the presence of *ca.* 2.5 and 5 Torr of  $\text{O}_2$  (curves B and C, respectively), in which DO is clearly re-formed. A potential explanation is given in Fig. 7 in which, following electrocyclic ring opening (step b), the radical formed can react with oxygen to form a di-carbonyl and  $\text{DO}_2$ . We note that our HONO source contains NO impurity and propose that the reformation of DO in this case arises as a result of reaction of  $\text{DO}_2$  with NO as shown. In the absence of  $\text{O}_2$ , the radical formed in step b can rearrange *via* H transfer (step c) to set up a conjugated single/double bond chain which, following ring closure and a 1,3 H-migration can form phenol and HO (step d). The net result of the above reaction scheme in the absence of  $\text{O}_2$  is therefore the thermodynamically favourable conversion of a heterocyclic five-membered,  $\text{C}_6\text{H}_6\text{O}$ , aromatic ring into a homonuclear six-membered aromatic ring of the same empirical formula.

However, in the absence of product data from the reaction, we emphasise that our discussion of the potential mechanism is necessarily rather speculative, and that other mechanisms to product formation (*e.g.*, addition of hydroxyl to other sites

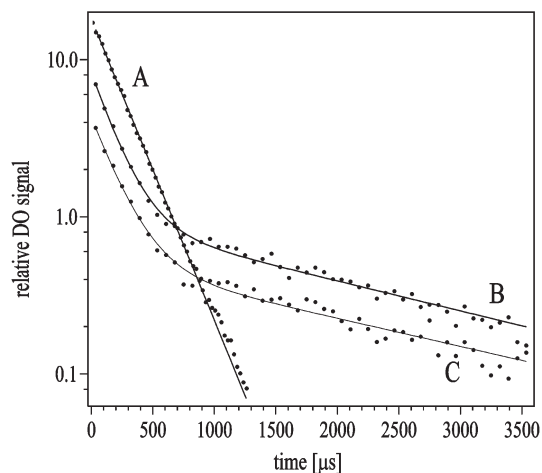


**Fig. 8** Decay of DO in the presence of  $4.6 \times 10^{14}$  molecules  $\text{cm}^{-3}$  2-vinylfuran, and various concentrations of  $\text{O}_2$ . Curve A:  $[\text{O}_2] = 0$ ; curve B:  $[\text{O}_2] = 2.5$  Torr; curve C:  $[\text{O}_2] = 5$  Torr. In all cases, the photolysis of DONO at 351 nm was used as a DO source. The drop in signal as  $\text{O}_2$  is progressively added, is due to quenching of the fluorescent DO ( $A^2\Sigma$ ) state.

on the aromatic ring, and also external to the ring) are certainly important. Product studies of the title reaction could shed light on these issues.

## Acknowledgements

We gratefully acknowledge the contribution of Elaine Fray and Charles Stirling at the Chemistry Department of the University of Sheffield (England) who synthesised the sample of 2-vinylfuran. The authors acknowledge the German Ministry of Education and Research (BMBF) for partial financial support within the COACH program. M.W. acknowledges support from the “Fonds der Chemischen Industrie”.

## References

- 1 V. A. Isidorov, I. G. Zenkevich and B. V. Ioffe, *Atmos. Environ.*, 1985, **19**, 1–8.
- 2 J. Williams, U. Pöschl, P. J. Crutzen, A. Hansel, R. Holzinger, C. Warneke, W. Lindinger and J. Lelieveld, *J. Atmos. Chem.*, 2001, **38**, 133–166.
- 3 I. T. Bertsch, R. J. Yokelson, D. E. Ward, T. J. Christian and W. M. Hao, *J. Geophys. Res.*, 2003, **108**, 8469.
- 4 T. E. Kleindienst, P. B. Shepson, E. O. Edney, L. D. Claxton and L. T. Cupitt, *Environ. Sci. Technol.*, 1986, **20**, 493–501.
- 5 F. Lipari, J. M. Dasch and W. F. Scruggs, *Environ. Sci. Technol.*, 1984, **18**, 326–330.
- 6 R. Atkinson, S. M. Aschmann, E. C. Tuazon, J. Arey and B. Zielinska, *Int. J. Chem. Kinet.*, 1989, **21**, 593–604.
- 7 M. Wollenhaupt, S. A. Carl, A. Horowitz and J. N. Crowley, *J. Phys. Chem. A*, 2000, **104**, 2695–2705.
- 8 A. Bierbach, I. Barnes and K. H. Becker, *Atmos. Environ.*, 1992, **26**, 813–817.
- 9 P. H. Wine and R. J. Thompson, *Int. J. Chem. Kinet.*, 1984, **16**, 867–878.
- 10 R. Atkinson, *Chem. Rev.*, 1986, **86**, 69–201.
- 11 A. Bierbach, I. Barnes and K. H. Becker, *Atmos. Environ.*, 1995, **29**, 2651–2660.
- 12 A. Alvarado, R. Atkinson and J. Arey, *Int. J. Chem. Kinet.*, 1996, **28**, 905–909.